Journal of Metals, Materials and Minerals, Vol.29 No.2 pp.64-69, 2019

Synthesis and luminescence properties of $CaMoO_4:Sm^{3+}$ phosphors for orange photonic materials

Narun LUEWARASIRIKUL[1,*], Jakrapong KAEWKHAO[2,3], and Hongjoo KIM[4]

[1]*Applied Physics Program, Faculty of Sciences and Technology, Suan Sunandha Rajabhat University, Bangkok, 10300, Thailand*
[2]*Physics Program, Faculty of Science and Technology, Nakhon Pathom Rajabhat University, Nakhon Pathom, 73000, Thailand*
[3]*Center of Excellence in Glass Technology and Materials Science (CEGM), Nakhon Pathom Rajabhat University, Nakhon Pathom, 73000, Thailand*
[4]*Department of Physics, Kyungpook National University, Daegu 702-701, Republic of Korea*

[*]**Corresponding author e-mail:** narun.lu@ssru.ac.th

Received date:
3 August 2018
Revised date:
5 October 2018
Accepted date:
27 October 2018

Keywords:
Phosphor
Samarium
Orange emission
Luminescence

Abstract

The series of $CaMoO_4$ samples with different melting temperature (600, 700, 800 and 900°C) were synthesized in this work to investigate their phase structures by X-ray diffraction (XRD). The XRD result confirmed that the crystalline structures of the phosphors were obtained at 800°C (tetragonal structure with $I4_{1/a}$ space group). Then, the series of $Ca_{1-x}MoO_4:Sm_x$ (where x = 0.005, 0.010, 0.015, 0.020, 0.025 and 0.030) were prepared by solid-state reaction method to study their luminescence properties. The absorption spectra, recorded in UV, Vis and NIR regions, showed peaks at 405, 465, 952, 1096, 1252, 1405, 1513, 1573 and 1629 nm. The excitation spectra, observed with 644 nm emission wavelength, showed the excitation peaks at 364, 377, 405, 419, 440, 481, 530 and 562 nm. The highest peak located at 405 nm corresponding to the $^6H_{5/2}\rightarrow{}^6P_{3/2}$ transition. The emission spectra, excited with 405 nm excitation wavelength, showed the emission peaks at 563, 605 and 644 nm, assigned as $^4G_{5/2}\rightarrow{}^6H_{5/2}$, $^6H_{7/2}$ and $^6H_{9/2}$ transitions, respectively. The concentration quenching of Sm^{3+} in the $Ca_{1-x}MoO_4:Sm_x$ phosphor occurred when x = 0.010. The emitted light of the phosphors, analyzed in the framework of the CIE 1931 color space, were shown in orange region.

1. Introduction

Nowadays, phosphors doped with rare earth ions have been widely used as luminescence materials for many photonic applications, such as lamp phosphors, cathode-ray tube phosphors, lasers, scintillators and light-emitting diodes, due to the intraconfigurational 4f-4f transitions characteristic of rare earth ions [1-2]. White light emitting diodes (w-LEDs) are the promising technology to replace the conventional fluorescent lighting technology because of many advantages, such as more energy-saving, long life-span, low-cost to prepare, more durability, lower melting temperature and better light quality (because of low ultraviolet and infrared radiation). White light emitting diodes generate white light by the combination of blue and yellow light from blue emitting LED chip and YAG:Ce3+ yellow emitting phosphor. However, this method has poor color rendering index (CRI) and high correlated color temperature (CCT) because of the lacking of red emitting component [3-6]. So, another method for generating white light is the combination of tricolor phosphors (red, green and blue).

Samarium ion (Sm^{3+}) is one of the most interesting rare earth ions due to its interesting optical properties, such as good emission in orange color, high luminescence efficiency and sharp luminescence pattern, which is useful for photonic materials [7-9]. Sm^{3+} ions, that exhibit sharp and strong emission peak around 550-700 nm, are suitable for using as the dopant for orange or orange-red emission phosphor used in w-LEDs applications [8-15].

Molybdate is the important optical materials that can be used in many applications. Molybdate is also used as a host material for phosphor because Mo metal ion is coordinated by four O^{2-} ions in tetrahedral symmetry that caused the MoO_4^{2-} is relatively stable. Many researches indicated that calcium molybdate ($CaMoO_4$) is one of the promising phosphor materials for using as photonic devices because $CaMoO_4$ is easy to prepare with low synthesizing temperature. Furthermore, $CaMoO_4$ exhibits good thermal and chemical stability and also has good luminescence properties [16-20].

In this work, the $CaMoO_4$ samples were synthesized with different melting temperature at 600, 700, 800 and 900°C to investigate their phase structures. Then, the series of $CaMoO_4$ phosphors doped with different concentration of Sm^{3+} with the composition of $Ca_{1-x}MoO_4:Sm_x$ (where x = 0.005, 0.010, 0.015, 0.020, 0.025 and 0.030) were synthesized to study their

DOI: 10.14456/jmmm.2019.20

absorption and luminescence properties. The appropriate melting temperature and the quenching effect of the Sm^{3+} concentration was studied in this work for determining the best synthesizing condition of the $CaMoO_4$ phosphors. The luminescence properties were studied for indicating that the CaMoO4 phosphors fabricated in this work were suitable for using in the w-LEDs applications.

2. Experimental

To determine the appropriate melting temperature of $CaMoO_4$ phosphors, the $CaMoO_4$ samples without doping Sm^{3+} were prepared by solid-state reaction method with different melting temperature (600, 700, 800 and 900°C) for 5 hours. Then, the $CaMoO_4$ doped with Sm^{3+} phosphors with the composition of $Ca_{1-x}MoO_4:Sm_x$ (where x = 0.005, 0.010, 0.015, 0.020, 0.025 and 0.030) were prepared by solid-state reaction method. Appropriate amounts of calcium carbonate ($CaCO_3$), molybdenum trioxide (MoO_3), and samarium (III) oxide (Sm_2O_3) were mixed and ground in an agate mortar before pressed with 20 tons by the hydraulic press machine. The mixtures were then melted in an electric furnace with the appropriate melting temperature for 5 hours. The $CaMoO_4:Sm^{3+}$ phosphors were labelled with the names as shown in Table 1.

Table 1. The phosphor samples.

Phosphor samples	Name
$Ca_{0.995}MoO_4:Sm_{0.005}$	CaMo:Sm05
$Ca_{0.99}MoO_4:Sm_{0.01}$	CaMo:Sm10
$Ca_{0.985}MoO_4:Sm_{0.015}$	CaMo:Sm15
$Ca_{0.98}MoO_4:Sm_{0.02}$	CaMo:Sm20
$Ca_{0.975}MoO_4:Sm_{0.025}$	CaMo:Sm25
$Ca_{0.97}MoO_4:Sm_{0.03}$	CaMo:Sm30

The crystalline structures of the phosphors were examined by X-ray diffractometer (Shimadzu, XRD-6001) with CuKα radiation (1.54 angstom). The data collected from 10° to 80° in 2θ range with a 0.02° scanning step. The absorption spectra were recorded in reflectance mode of UV-Vis-NIR spectrophotometer (Shimadzu, UV-3600). The luminescence spectra (excitation spectra, emission spectra and luminescence decay time) were measured by fluorescence spectrophotometer (Agilent, Cary Eclipse). The color of the emitted light was evaluated in the framework of the CIE 1931 chromaticity diagram.

3. Results and discussion

3.1 Structure characterization

In order to determine the appropriate melting temperature of $CaMoO_4$ phosphors in this work, the $CaMoO_4$ samples without doping Sm^{3+} were synthesized with different melting temperature (600, 700, 800 and 900°C) for 5 hours. The XRD results (Figure 1) show that the phase structure of the phosphor synthesized at 600°C does not match the crystalline structure of $CaMoO_4$ (JCPDS card No. No.29-0351). The characteristic peaks of $CaMoO_4$ phases appear when the melting temperature more than 700°C. The diffraction peaks with the strongest intensities appear at 800°C melting temperature. At 800°C, the diffraction pattern of all peaks can be attributed to the tetragonal $CaMoO_4$ phase and no other impurity peaks are indexed. The result shows that 800°C is the appropriate melting temperature for fabricating the $CaMoO_4$ phosphors in this work. Figure 2 shows the XRD spectra of the $Ca_{1-x}MoO_4:Sm_x$ (where x = 0.005, 0.010, 0.015, 0.020, 0.025 and 0.030) phosphors synthesized at 800°C for 5 hours. The result shows that the crystalline structures of all samples show no significant change. This result implies that Sm^{3+} ions were completely doped into the $CaMoO_4$ lattices without making a significant change to the crystalline structure [16,19].

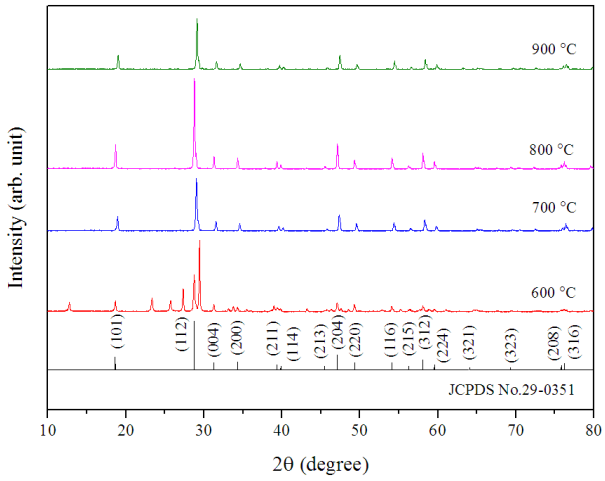

Figure 1. The XRD spectra of the $CaMoO_4$ phosphors synthesized at different temperatures.

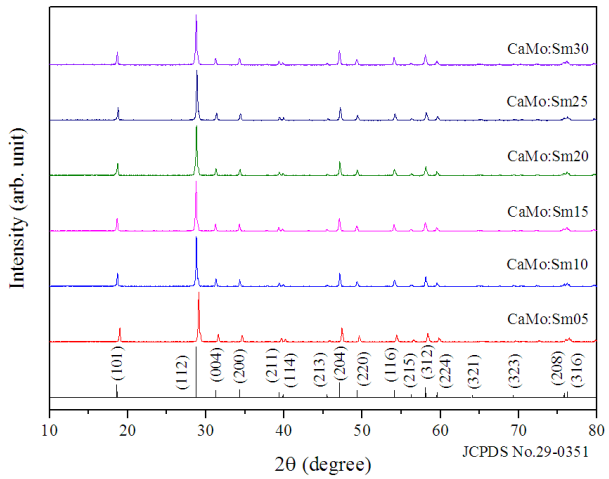

Figure 2. The XRD spectra of the $CaMoO_4:Sm^{3+}$ phosphors.

3.2 Absorption spectra

Figure 3 shows the absorption spectra recorded in reflectance mode of the CaMo:Sm30 phosphor in UV-Vis and NIR region. The absorption bands show the peaks at 405 and 465 nm in UV-Vis region corresponding to the $^6H_{5/2}\rightarrow{}^6P_{3/2}$ and $^6H_{5/2}\rightarrow{}^4I_{11/2}$ transitions, respectively, and show the peaks at 952, 1096, 1252, 1405, 1513, 1573, 1629 nm in NIR region corresponding to the $^6H_{5/2}\rightarrow{}^6F_{11/2}$, $^6F_{9/2}$, $^6F_{7/2}$, $^6F_{5/2}$, $^6F_{3/2}$, $^6H_{15/2}$ and $^6H_{13/2}$ transitions, respectively [6-9]. The strongest absorption in UV-Vis region occurs at 405 nm ($^6H_{5/2}\rightarrow{}^6P_{3/2}$ transition).

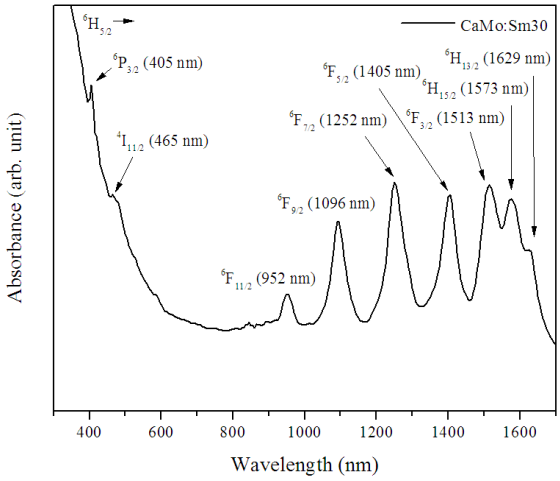

Figure 3. The absorption spectra of the CaMo:Sm30 phosphor in UV-Vis-NIR region.

3.3 Luminescence properties

The excitation and emission spectra of the $CaMoO_4:Sm^{3+}$ phosphors are shown in Figure 4 and Figure 5, respectively. The excitation spectra, observed with 644 nm emission wavelength, show peaks centered at 364, 377, 405, 419, 440, 481, 530 and 562 nm, corresponding to the $^6H_{5/2}\rightarrow{}^4D_{3/2}$, $^6P_{7/2}$, $^6P_{3/2}$, $^4P_{5/2}$, $^4G_{9/2}$, $^4I_{11/2}$, $^4F_{3/2}$ and $^4G_{5/2}$ transitions, respectively [7-8]. The highest peak belongs to the $^6H_{5/2}\rightarrow{}^6P_{3/2}$ transition at 405 nm. The emission spectra, excited with 405 nm excitation wavelength, show the emission bands centered at 563, 605 and 644 nm, corresponding to the $^4G_{5/2}\rightarrow{}^6H_{5/2}$, $^6H_{7/2}$ and $^6H_{9/2}$ transitions, respectively [7-8]. The emission peak of the $^4G_{5/2}\rightarrow{}^6H_{7/2}$ transition is split into two peaks because of the crystal-field splitting [21]. The splitting of the $^4G_{5/2}\rightarrow{}^6H_{7/2}$ emission peak of phosphors doped with Sm^{3+} can also be found in many reports [17,22-23]. From the emission spectra, the $^4G_{5/2}\rightarrow{}^6H_{5/2}$ transition (563 nm) is corresponding to the magnetic dipole (MD) allowed transition that the intensity of the MD allowed transition is independent from crystal field effect. The $^4G_{5/2}\rightarrow{}^6H_{7/2}$ transition (605 nm) is partly magnetic dipole (MD) and partly electric dipole (ED) allowed transition. And the $^4G_{5/2}\rightarrow{}^6H_{9/2}$ transition (644 nm) is purely electric dipole (ED) crystal field sensitive transition [4-5]. The intensity ratio of ED to MD can be used to determine the asymmetric nature of the sites around RE^{3+} ions, so the more ED/MD ratio indicates the more asymmetric nature sites around RE^{3+} ions. In this work, the ED/MD ratios are found to be 4.87, 5.53, 4.81, 4.50, 4.54 and 4.47 for the CaMo:Sm05, CaMo:Sm10, CaMo:Sm15, CaMo:Sm20, CaMo:Sm25 and CaMo:Sm30 phosphors, respectively. This result indicates that all the samples have high asymmetric sites occupied by Sm^{3+} ions. The x,y color coordinates of emitted light, evaluated in the framework of the CIE 1931 chromaticity diagram, of all samples are all located in orange region with the coordinate (0.61, 0.38). Figure 6 shows the location of x,y color coordinate of the samples on CIE 1931 chromaticity diagram.

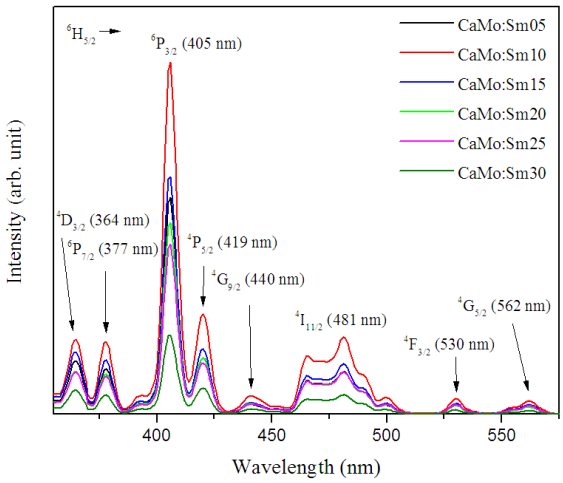

Figure 4. The excitation spectra of the $CaMoO_4:Sm^{3+}$ phosphors observed with 600 nm.

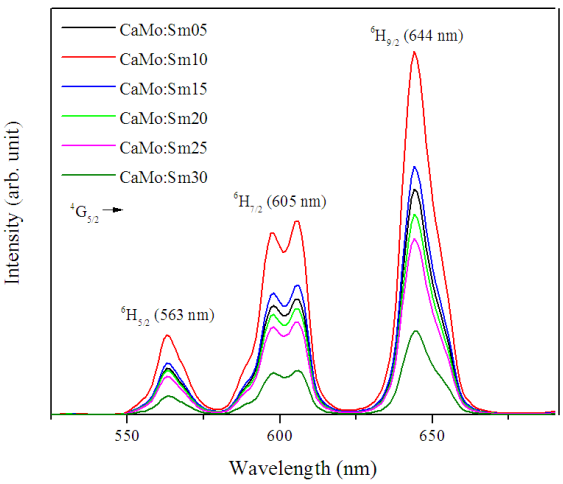

Figure 5. The emission spectra of the $CaMoO_4:Sm^{3+}$ phosphors excited by 400 nm.

Figure 4 and Figure 5 show that the intensities of both excitation and emission peaks are increasing when the concentration of Sm^{3+} increases from 0.005

up to 0.010, then the intensities turn to decrease when Sm^{3+} more than 0.010 due to the concentration quenching effect. Thus, the optimized concentration of Sm^{3+} doped in the $CaMoO_4:Sm^{3+}$ phosphors in this work is 0.010. The concentration quenching effect occurs because the more Sm^{3+} ions contained in the phosphor, the more energy transfer process between Sm^{3+} ions occurs. With the increasing of Sm^{3+} concentrations, the energy stages of Sm^{3+} are close together to interact and the strong interaction between Sm^{3+} ions are able to transfer the non-radiative energy. And the more non-radiative energy process leads to the lower of luminescent intensity. So the $Ca_{0.99}MoO_4:Sm_{0.01}$ phosphor gives the highest light yield [4-5].

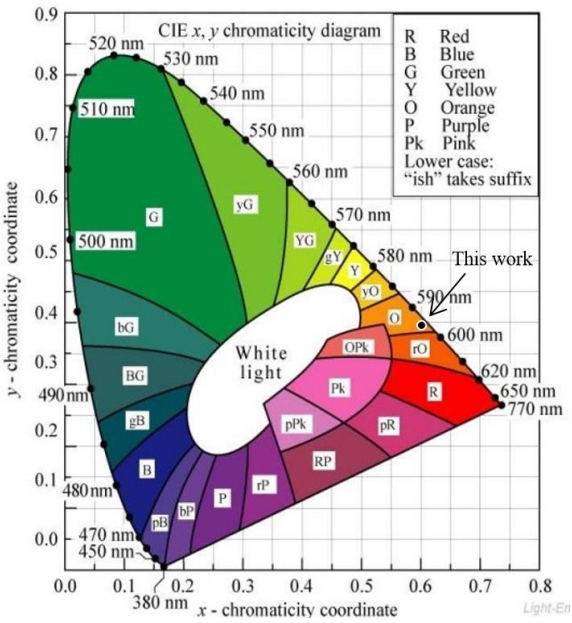

Figure 6. The CIE 1931 diagram of the $CaMoO_4:Sm^{3+}$ phosphors.

Table 2. The decay times for all emission peaks of the phosphor samples.

Phosphor samples	Decay time (ms)		
	$^4G_{5/2}\rightarrow{}^6H_{5/2}$ transition	$^4G_{5/2}\rightarrow{}^6H_{7/2}$ transition	$^4G_{5/2}\rightarrow{}^6H_{9/2}$ transition
CaMo:Sm05	0.520	0.525	0.525
CaMo:Sm10	0.510	0.514	0.515
CaMo:Sm15	0.501	0.503	0.502
CaMo:Sm20	0.486	0.488	0.485
CaMo:Sm25	0.427	0.431	0.430
CaMo:Sm30	0.422	0.422	0.425

The luminescence decay time had been measured by exciting the Sm^{3+} ions in phosphors to the $^6P_{3/2}$ level with 405 nm excitation wavelength, then observing the $^4G_{5/2}\rightarrow{}^6H_{5/2}$, $^6H_{7/2}$ and $^6H_{9/2}$ transitions with 563, 605 and 644 nm emission, respectively. The decay times for all emission peaks are reported in Table 2. The results show that the decay times for all emission peaks decrease when increasing the concentration of Sm^{3+} due to the increasing of energy transfer process between Sm^{3+} ions. The decay profile curves of the $^4G_{5/2}\rightarrow{}^6H_{9/2}$ transition emission are found to be single exponential for all samples, as shown in Figure 7.

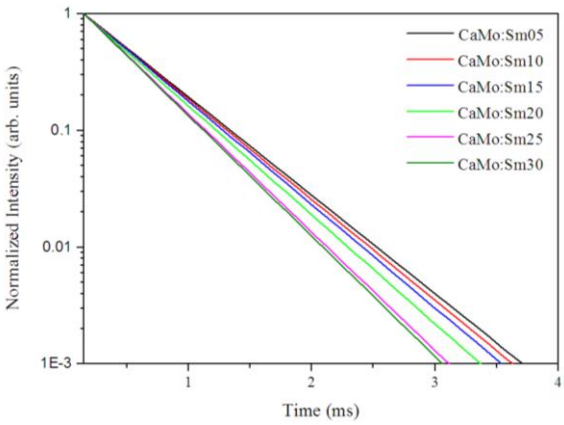

Figure 7. The decay curve of the $CaMoO_4:Sm^{3+}$ phosphors for the $^4G_{5/2}\rightarrow{}^6H_{9/2}$ transition.

4. Conclusions

In this work, the $CaMoO_4:Sm^{3+}$ phosphors were prepared by solid-state reaction with their appropriate melting temperature at 800°C for 5 hours. The XRD spectra show that the crystalline structure has no significant changes when increasing the Sm^{3+} concentration. The result implies that Sm^{3+} ions were completely doped into the $CaMoO_4$ lattices without making significant changes to the crystalline structure. The absorption spectra show the strongest absorption peak in UV-Vis region at 405 nm (corresponding to the $^6H_{5/2}\rightarrow{}^6P_{7/2}$ transition). The excitation spectra, observed with 644 nm emission wavelength, show peaks centered at 364, 377, 405, 419, 440, 481, 530 and 562 nm. The highest excitation peak belongs to the $^6H_{5/2}\rightarrow{}^6P_{3/2}$ transition at 405 nm. The emission spectra show the emission bands at 563, 605 and 644 nm. The ED/MD ratios show that all the samples have high asymmetric sites occupied by Sm^{3+} ions. The x,y color coordinates of all samples are all located in orange region. The decay times for all emission peaks decrease when increasing the concentration of Sm^{3+} due to the increasing of energy transfer process between Sm^{3+} ions. The $Ca_{0.99}MoO_4:Sm_{0.01}$ phosphor gives the highest emission light yield due to the concentration quenching effect. The results show that the $CaMoO_4:Sm^{3+}$ phosphors in this work are suitable for using in w-LEDs applications and also suitable for using as the orange photonic material.

5. Acknowledgements

The authors would like to thanks Suan Sunandha Rajabhat University (SSRU) and Center of

Excellence in Glass Technology and Materials Science (CEGM), Nakhon Pathom Rajabhat University (NPRU) for supporting this research.

References

[1] G. K. Ribeiro, F. S. Vicente, M. I. B. Bernardi and A. Mesquita, "Short-range structure and photoluminescent properties of the $CaTiO_3$:Pr,La phosphor," *Journal of Alloys and Compounds*, vol. 688, pp. 497-503, 2016.

[2] J. Fu, Q. Zhang, Y. Li, and H. Wang, "Highly luminescent red light phosphor $CaTiO_3:Eu^{3+}$ under near-ultraviolet excitation," *Journal of Luminescence*, vol. 130, pp. 231-235, 2010.

[3] H. Li, X. Gong, Y. Chen, J. Huang, Y. Lin, Z. Luo, and Y. Huang, "Luminescence properties of phosphate phosphors $Ba_3Gd_{1-x}(PO_4)_3:xSm^{3+}$," *Journal of Rare Earths*, vol. 36, pp. 456-460, 2018.

[4] J. Li, R. Pang, Z. Yu, L. Liu, H. Wu, H. Li, L. Jiang, S. Zhang, J. Feng, and C. Li, "Preparation and luminescence properties of orange-red $Ba_3Y_4O_9:Sm^{3+}$ phosphors," *Journal of Rare Earths*, vol. 36, pp. 680-684, 2018.

[5] S. Kaur, A. S. Rao, and M. Jayasimhadri, "Spectroscopic and photoluminescence characteristics of Sm^{3+} doped calcium aluminozincate phosphor for applications in w-LED," *Ceramics International*, vol. 43, pp. 7401-7407, 2017.

[6] Q. Yang, G. Lia, Y. Wei, and H. Chai, "Synthesis and photoluminescence properties of red-emitting $NaLaMgWO_6:Sm^{3+},Eu^{3+}$ phosphors for white LED applications," *Journal of Luminescence*, vol. 199, pp. 323-330, 2018.

[7] C. Madhukar Reddy, B. Deva Prasad Raju, N. John Sushma, N. S. Dhoble and S. J. Dhoble, "A review on optical and photoluminescence studies of RE^{3+} (RE=Sm, Dy, Eu, Tb and Nd) ions doped LCZSFB glasses," *Renewable and Sustainable Energy Reviews*, vol. 51, pp. 566-584, 2015.

[8] R. Vijaya, V. Venkatramu, P. Babu, C. K. Jayasankar, U. R. Rodriguez-Mendozad and V. Lavin, "Spectroscopic properties of Sm^{3+} ions in phosphate and fluorophosphate glasses," *Journal of Non-Crystalline Solids*, vol.365, pp. 85-92, 2013.

[9] J. Zhang, C. Chen, X. Zhang, X. Wang, W. Shi and B. Han, "Photoluminescence properties of Sm^{3+} doped barium borophosphate phosphors," *Optik*, vol. 158, pp. 1499-1503, 2018.

[10] J. Wu, M. Li, M. Wang, Z. Liu and H. Jia, "Preparation and luminescence properties of $NaLa(WO_4)_2:Sm^{3+}$ orange-red phosphor," *Journal of Luminescence*, vol. 197, pp. 219-227, 2018.

[11] B. Ramesh, G.R. Dillip, G. Rajasekhara Reddy, B. Deva Prasad Raju, S.W. Joob, N. John Sushmad and B. Rambabue, "Luminescence properties of $CaZn_2(PO_4)_2:Sm^{3+}$ phosphor for lighting application," *Optik*, vol. 156, pp. 906-913, 2018.

[12] L. Wang, H. Mi Noh, B. K. Moon, B. C. Choi, J. H. Jeong and J. Shi, "Luminescent properties and energy transfer of Sm^{3+} doped $Sr_2CaMo_{1-x}W_xO_6$ as a potential phosphor for white LEDs," *Journal of Alloys and Compounds*, vol. 663, pp. 808-817, 2016.

[13] L. Li, S. Fu, Y. Zheng, C. Li, P. Chen, G. Xiang, S. Jiang and X. Zhou. "Near-ultraviolet and blue light excited Sm^{3+} doped Lu_2MoO_6 phosphor for potential solid state lighting and temperature sensing," *Journal of Alloys and Compounds*, vol. 738, pp. 473-483, 2018.

[14] X. Zhang, Y. Li, R. Hu, Z. Xu, J. Qiu, Z. Yang and Z. Song, "Color tunable and white light emitting via energy transfer in single-phase $BiOCl:Er^{3+},Sm^{3+}$ phosphors for WLEDs," *Journal of Rare Earths*, vol. 36, pp. 231-237, 2018.

[15] A.N. Meza-Rocha, S. Bordignon, A. Speghini, R. Lozada-Morales and U. Caldino, "Zinc phosphate glasses activated with $Dy^{3+}/Eu^{3+}/Sm^{3+}$ and $Tb^{3+}/Eu^{3+}/Sm^{3+}$ for reddish-orange and yellowish white phosphor applications," *Journal of Luminescence*, vol. 203, pp. 74-82, 2018.

[16] Y. Zhai, Y. Han, W. Zhang, Y. Yin, X. Zhao, J. Wang and X. Liu, "Influence of doping alkali metal ions on the structure and luminescent properties of microwave synthesized $CaMoO_4:Dy^{3+}$ phosphors," *Journal of Alloys and Compounds*, vol. 688, pp. 241-247, 2016.

[17] A. A. Ansi, M. Alam, "Optical and structural studies of $CaMoO_4$:Sm, $CaMoO_4$:Sm@$CaMoO_4$ and $CaMoO_4$:Sm@$CaMoO_4$@SiO_2 core-shell nanoparticles," *Journal of Luminescence*, vol. 157, pp. 257-263, 2015.

[18] F. Kang, Y. Hu, H. Wu, G. Ju, Z. Mu and N. Li, "Luminescence investigation of Eu^{3+}-Bi^{3+} co-doped $CaMoO_4$ phosphor," *Journal of Rare Earths*, vol. 29, pp. 837-842, 2011.

[19] G. Li, G. Jia, B. Yang, X. Li, L. Jin, Z. Yang and G. Fu, "Synthesis and optical properties of Dy^{3+}, Li^{3+} doped $CaMoO_4$ phosphor," *Journal of Rare Earths*, vol. 29, pp. 540-543, 2011.

[20] F. Kang, Y. Hu, H. Wu, G. Ju, Z. Mu and N. Li, "Luminescent properties and energy transfer mechanism from Tb^{3+} to Eu^{3+} in $CaMoO_4:Tb^{3+},Eu^{3+}$ phosphors," *Journal of Rare Earths*, vol. 34, pp. 251-258, 2016.

[21] S. Pikker, L. Dolgov, S. Heinsalu, S. Mamykin, V. Kiisk, S. Kopanchuk, R. Lohmus and I. Sildos, "Gilded nanoparticles for plasmonically enhanced

fluorescence in $TiO_2:Sm^{3+}$ sol-gel films," *Nanoscale Research Letters*, vol. 9:143, pp.1-6, 2014.

[22] A. Kuzmanoski, V. Pankratov and C. Feldmann, "Microwave-assisted ionic-liquid-based synthesis of highly crystalline $CaMoO_4:RE^{3+}$ (RE = Tb, Sm, Eu) and $Y_2Mo_4O_{15}:Eu^{3+}$ nanoparticles," *Solid State Sciences*, vol. 41, pp. 56-62, 2015.

[23] J. Zhang, L. Wang, Y. Jin, X. Zhang, Z. Hao and X. Wang, "Energy transfer in $Y_3Al_5O_{12}:Ce^{3+}$, Pr^{3+} and $CaMoO_4:Sm^{3+}$, Eu^{3+} phosphors," *Journal of Luminescence*, vol. 131 (3), pp. 429-432, 2011.